Astronomical and Astrophysical Transactions (*AApTr*), 2025, Vol. 35, Issue 2, pp. 135–146,
ISSN 1055-6796, Photocopying permitted by license only, ©Cambridge Scientific Publishers

A comprehensive study of spectroscopic binary Cepheids in the Gaia epoch

A.S. Rastorguev[1,3,*], M.V. Zabolotskikh[3], N.N. Samus[2,3], N.A. Gorynya[2,3]

[1] *Faculty of Physics, Lomonosov Moscow State University, Moscow, 119991 Russia*
[2] *Institute of Astronomy, Russian Academy of Sciences, Moscow, 119017 Russia*
[3] *Sternberg State Astronomical Institute, Lomonosov Moscow State University, Moscow, 119992 Russia*

Received 27 April, 2025; accepted 29 May, 2025

The results of the Gaia mission, primarily precision astrometric measurements of trigonometric parallaxes and proper motions, as well as photometric measurements in two bands, provide a significant expansion of the possibilities for a comprehensive study of spectroscopic binary Cepheids. Long-term measurements of radial velocities allow us not only to determine the parameters of the relative orbits of the Cepheids, but also to determine the pulsation radii of Cepheids, to refine their luminosities and evolutionary stages. Calculations of Galactic orbits of these systems carry additional information about the membership of Cepheids in different stellar populations of the Galaxy. The successes of the comprehensive study of such objects are discussed on the example of the spectroscopic binary Cepheids V350 Sgr, AU Peg, and TX Del.

Keywords: Spectroscopic binary stars, variable stars, Cepheids, stellar evolution

1 Introduction

Spectroscopic binary Cepheids are a natural laboratory for a comprehensive study of the population of pulsating variable stars. The orbital parameters calculated from radial velocities of the Cepheids, in particular, their mass function, allow us to make dynamical estimates of the satellite masses, and, in the presence of additional data on the physical characteristics of the satellite, even to estimate the masses of the Cepheids themselves. Together with pulsation estimates of their radii, these data allow us to clarify the evolutionary stage of Cepheid and its position in the instability strip. Obviously, the clarification of the evolutionary status of Cepheids can in principle refine the parameters of the "period–luminosity" relation. Spectroscopic binary Cepheids have become one of the main goals of the more than 30-year campaign of measurements of radial velocities of about 160 cepheids in the northern sky with a

*Email: alex.rastorguev@gmail.com

correlation spectrograph – the Radial Velocity Meter (RVM) (Tokovinin 1987), jointly conducted by INASAN and SAI MSU. From 1987 to 2022, more than 14000 radial velocities with a characteristic accuracy of about 0.3–0.5 km/s have been measured within the framework of this program (Gorynya et al. 1992, 1996, 1998).

In this paper, using three spectroscopic binary Cepheids as examples, we show that the use of additional research methods and new astrometric and photometric data from the Gaia DR3 mission can provide valuable information and significantly refine some astrophysical parameters and the classification of Cepheids (Gaia Collaboration 2018, 2021, 2016, 2023).

2 Three spectroscopic binary Cepheids

2.1 V350 Sgr classical Cepheid

Classical Cepheid V350 Sgr (Gaia EDR3 4080122796947250176) has been studied in many papers. Its orbital period was estimated from RVM measurements and other spectroscopic data as $P_{orb} \approx 1467^d$ (Evans and Sugars 1997, Gorynya et al. 1995). In the papers of Evans (2013), Evans et al. (2011, 1997), spectroscopic observations made by the IUE and HST space missions in the FUV bands (184–188 nm, 132–151 nm) were used to directly observe the companion, B8V-B9V star, and to measure mass ratio of two components. Based on HST observations made in 2013 and 2016 in two orbital phases at a velocity difference of $\Delta V \approx -43.0 \pm 1.9$ km/s, close to their maximum difference, the most reliable estimate of the mass of V350 Sgr was obtained: $M_{cep} \approx 5.2 \pm 0.3\ M_\odot$ (Evans et al. 2018).

To refine the parameters of V350 Sgr and its evolutionary status, we decided to calculate the pulsation radius, to use Gaia photometric and astrometric data and MESA evolutionary tracks (Dotter 2016). First of all, we obtained the pulsation velocity curve by standard decomposition of measured radial velocity into the contributions of Keplerian orbital motion and pulsations described in the form of the trigonometric expansion by the pulsation phase. We also used the "temperature" method originated from Rastorguev et al. (2022) to calculate mean radius and radius variations as well as M_V and M_{bol} absolute magnitude light curves. To determine the mean radius, we used 145 light measurements in bands (B, V, I) from the Berdnikov's database (see references in Evans et al. (2011)) in JD intervals quasi-synchronous with the radial velocity measurements. All photometric data were previously corrected for the contribution of the companion star $B8V$–$B9V$. It turns out that our derived value of $\langle M_V \rangle_I \approx (-3.64 - -3.57)$ mag, and the distance $D \approx 980$–993 pc for V350 Sgr are in much better agreement with the estimate made with Bayesian distance $rgeo$ taken from the Gaia DR2 catalog (Bailer-Jones et al. 2018) than with later determinations in Gaia DR3. The mean radius of the Cepheid $\langle M_V \rangle_I \approx 42$–$43 R_\odot$ with the radius variations about $\pm 1 R_\odot$ (Rastorguev et al. 2024b). Figure 1 demonstrates the position of V350 Sgr on HR diagram with the parameters calculated by our "temperature" method. The best agreement is obtained for masses of 5.1–5.2 $M_\odot$ and $[Fe/H] \approx -0.18, -0.10$, respectively. Blue loops of the evolutionary tracks for $[Fe/H] \approx 0, +0.15$ are too short and these variants can be certainly excluded. Based on our calculations and the position of V350 Sgr on HRD, we can reduce the

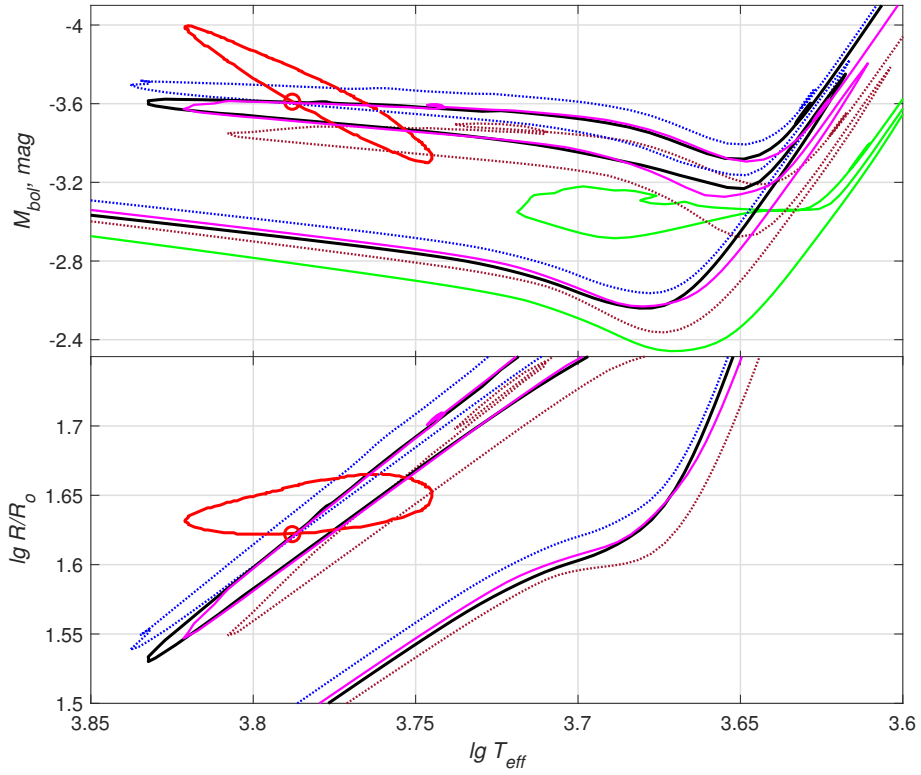


Figure 1 HRD for V350 Sgr. The dotted blue line is the evolutionary track of MESA (Dotter 2016), calculated for a star with mass $5.2M_{\odot}$ and $[Fe/H] = -0.18$ dex. The solid black line and the nearly matching solid pink line are tracks for stars with masses $5.1M_{\odot}$ and $[Fe/H] = -0.18$ dex and $5.2M_{\odot}$ and $[Fe/H] = -0.10$ dex, respectively. The dotted brown line and the solid green line show the tracks for a star with mass $5.2M_{\odot}$ and $[Fe/H] = 0.00, +0.15$ dex, respectively, for comparison. The solid red ellipses – calculated pulsation "tracks" of the Cepheid in ($\lg T_{\rm eff}$, M_{bol}, $\lg R/R_{\odot}$) coordinate space. The small red circle shows the flux-averaged values of the effective temperature, radius and the luminosity. Top: ($\lg T_{\rm eff} - M_{bol}$) diagram; bottom: ($\lg T_{\rm eff} - lgR/R_{\odot}$) diagram. The position of the star on the evolutionary tracks corresponds to an age of about 100 Myr at the 3rd crossing of the instability strip with secular increase in P_{pls}.

interval of its mass estimates to 5.1–5.2 $M_{\odot}$. Calculation of orbital parameters gives also the value of the mass function $f(M)$. Knowing the masses of the Cepheid and its companion, we can directly estimate the orbital inclination angle and the absolute size of the major semi-axis of the relative orbit: from

$$f(M) = \frac{M_2^3 \cdot \sin^3 i}{(M_1 + M_2)^2} = 1.0385 \cdot 10^{-7} \cdot (1 - e^2)^{3/2} \cdot K_1^3 \cdot P\ (M_{\odot}) \approx (0.137 \pm 0.004) M_{\odot}$$

we can estimate $i \approx (53 \pm 3)^{\circ}$, $a \approx (5 \pm 0.1)$ A.U.

2.2 T2 Cepheid AU Peg

The unique spectroscopic binary cepheid AU Peg (Gaia DR3 1785352625740690432) with the shortest orbital period $P_{orb} \approx 53.3^d$ was discovered by Hoffmeister (1930) and subsequently assigned to type II (T2) Cepheids, of BL Her subtype. This subtype includes low mass variable stars on the evolutionary stage of the instability strip crossing from the horizontal branch to the asymptotic giant branch (AGB). Soszyński et al. (2017a,b, 2018) assigned to this subtype the T2 Cepheids with periods ranging from 1 to 4–5^d observed by the OGLE project (Udalski et al. 2015) in the LMC, SMC, and in Milky Way bulge. Pulsation models of stars at this stage for masses 0.5–0.65 $M_\odot$ and metallicities $Z = 0.0001, 0.001, 0.004$ were calculated by Marconi and Di Criscienzo (2007), and later by Das et al. (2021, 2024) for wider range of masses (0.5–0.8 $M_\odot$), metallicities ($-2.0 < [Fe/H] < 0.0$), and luminosities (50–300 $L_\odot$).

Harris et al. (1984) and Vinko et al. (1993) based on erroneous distance data significantly overestimated AU Peg luminosity. They also noted its unusual red color and placed the star beyond the red boundary of the instability strip. They also noted that the companion mass is larger than that of Cepheid, due to past mass exchange, and concluded that the radius of the star may be close to the filling Roche limit.

We decided to revise AU Peg's radius, mass, and evolutionary status based on our new measurements of radial velocities, photometry, and Gaia DR3 astrometry. Our 53 radial velocity measurements were made in the interval JD 2455492–2459490 simultaneously with the 44 brightness measurements in the (G, BP, RP) bands of Gaia DR3 (JD 2456962–2457877) (VizieR Online Data Catalog I/355/epphot). The simultaneous spectroscopic and photometric measurements are necessary to eliminate possible systematic errors in the determination of the pulsation radii of the Cepheids. The radial velocity and photometry series at these time intervals are well described by a common value of the pulsation period $P_{pls} \approx 2.4125^d$. We calculated the orbital parameters of AU Peg, including mass function $f(M) \approx (0.52 \pm 0.02) M_\odot$ and $a_1 \cdot \sin\, i \approx (0.220 \pm 0.002)$ A.U. by solving standard Kepler orbit. The decomposition of radial velocity onto the orbital and pulsation contributions is shown on left and right upper panels of Fig. 2, respectively.

We used a generalization of the Balona (1977) method to estimate the radius variations, consisting in representing the observed light curve in a general form suitable for any pair of temperature sensitive photometric bands:

$$Magn = -5 \cdot \lg[\langle R \rangle + r(phase)] + \sum_{k=1}^{K} a_k \cdot CI^k + C,$$

where $Magn$ is the apparent magnitude of the star, CI is the observed color index, a_k), C are constants, $\langle R \rangle$ is the mean radius, $r(phase)$ is its variation with phase. A significant advantage of this technique over the surface brightness method of Barnes and Evans (1976), Barnes et al. (1978) is that we can use the light and color curves not corrected for absorption. As shown by Rastorguev and Dambis (2011), all absorption information is included in the constant C. From this, we estimate AU Peg radius as $\langle R \rangle / R_\odot \approx 16.0 \pm 0.6$, with an amplitude of about $\pm 0.7 R_\odot$.

In analyzing G light curve, we detected for the first time almost sinusoidal variations with a half orbital period of 26.6653 day at the level of $\Delta G \approx 0.02$ mag (as shown at the bottom left in Fig. 2). Given the short orbital period of AU Peg and the

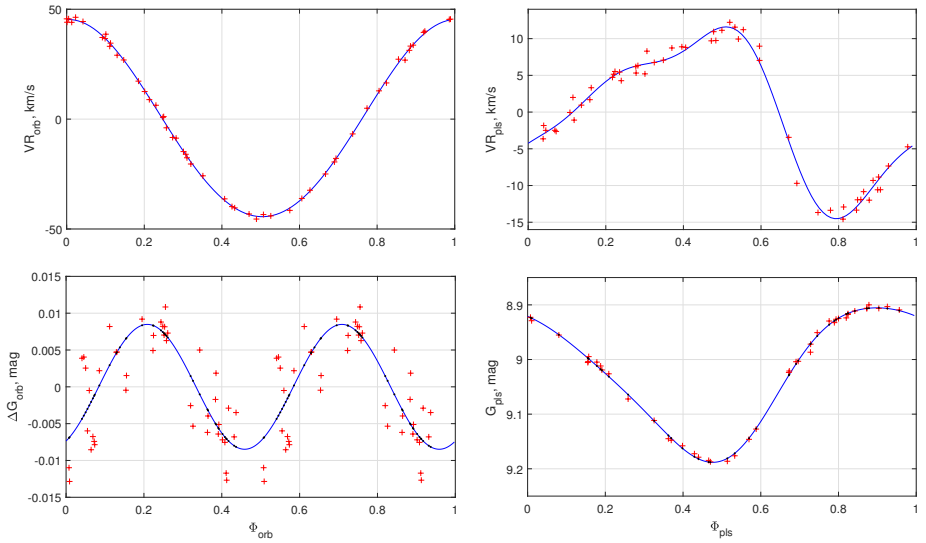


Figure 2 Top: decomposition of the AU Peg radial velocity into orbital motion (left) and pulsation (right) contributions. Bottom: decomposition of the light curve in the G band from Gaia DR3 data. On the left are the light changes due to the ellipsoidality effect at ± 0.01 mag with a period equal to half the orbital period (26.6653^d). On the right is the light curve in the G band ($P_{pls} = 2.4125$ days). All phases are counted from the moment $T_0 = JD$ 2450090.895.

presence of a more massive companion, we can confidently interpret the light variations we discovered as a manifestation of the effect of the ellipsoidality of binary's main component. Light variations are synchronized with the orbital phases: in the quadrature phases Cepheid is systematically brighter than in conjunction phases: in quadratures, the lateral surface of the star's elongated spheroid is projected onto the celestial sphere, while in conjunctions its frontal cross section is projected. Obviously, the observed ellipsoidality effect is associated with Cepheid's tidal interaction with its companion, and this imposes additional constraints on the mass ratio of the components and the inclination angle of the relative orbit to the celestial plane, and allows us to somewhat clarify the evolutionary status of the system (Rastorguev et al. 2024a).

To estimate the contribution of the ellipsoidality effect to the total flux, we used an approximation for the shape of the star as an elongated spheroid and the expressions for the projections of this spheroid onto celestial plane (all references are taken from Cherepashchuk (2013)). We also used our estimates of $f(M)$ and $a_1 \cdot \sin\ i$. The family of curves calculated for different inclination angles i shows how the ellipsoidality effect depends on the Cepheid's mass, M_1 (lower right panel of Fig. 3); black horizontal line marks the observed value of $\Delta G \approx 0.02$ mag. We can estimate a lower and upper limit for the possible Cepheid's mass as $0.65 \leq M_1/M_\odot \leq 0.85$ based on the intersection of these curves with the observed ΔG limit. The characteristic error of the mass boundaries due to different sources of uncertainties is about $0.05 M/M_\odot$. It is easy to see from the diagrams that the minimum mass of the Cepheid's companion should be

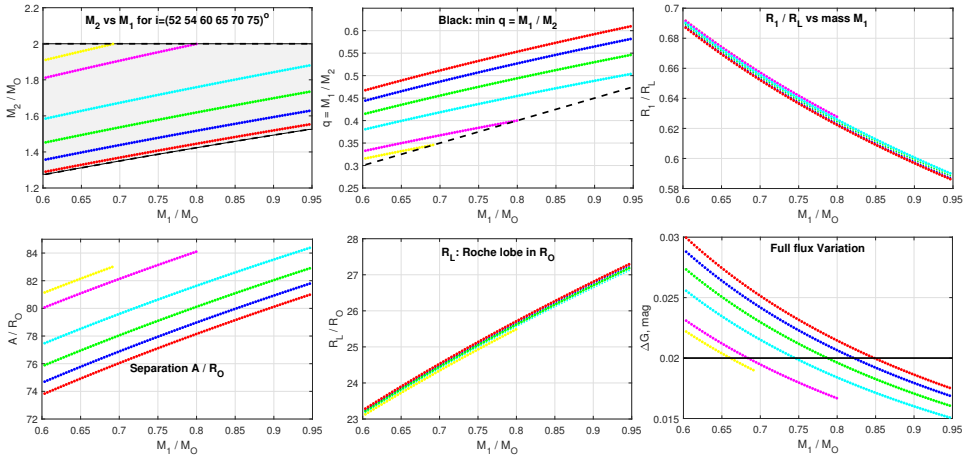


Figure 3 Diagnostic diagrams for AU Peg show the dependencies of the companion's mass M_2, mass ratio M_1/M_2, Roche lobe radius $R_L/R_\odot$, degree of Roche lobe filling, component's spacing $A/R_\odot$, ellipsoidality effect ΔG on the Cepheid's mass for a set of orbital plane inclination angles $i = (52, 54, 60, 65, 70, 75)^\circ$. The lower black dashed line in the upper left panel bounds the "forbidden zone" in which mutual eclipses of the components are possible. The "permitted" tilt angles are $i \leq 75^\circ$. The upper dashed line in this diagram corresponds to the maximum mass of the satellite at which it makes a major contribution to the brightness of the total system. The black solid line in the lower right panel indicates the observed level of variability due to the ellipsoidality effect, $\Delta G \approx 0.02$ mag.

about $M_2(min)/M_\odot \approx 1.50 \pm 0.05$. Note also that taking into account the companion's contribution to the integral brightness of the system will lead to some increase in ΔG caused by the ellipsoidality of the main component and, in turn, to a lowering of the upper limit of its mass. After accounting for the satellite's contribution to the total system brightness, estimates of the mean radius of the Cepheid increase to about 16.7 $R_\odot$. The cepheid fills the Roche lobe by about 60–70%, as can be seen from upper right panel on Fig. 3.

Recent mass ratio $M_2/M_1 > 1.7$; so the system experienced a mass exchange some times ago, and the more massive component, having lost a significant part of its mass, became a subgiant with a mass less than ∼0.85–0.9 $M_\odot$. The present total system mass is, as follows from our results, (2.4–2.6) $M_\odot$. Therefore, the initial mass of the main component of the system could in no way be less than half of the present total mass, i.e., ∼(1.2–1.3) $M_\odot$. The MESA (Dotter 2016) evolutionary tracks for $[Fe/H] \sim +0.1$ *dex* predict an evolutionary time for stars with initial masses (1.2, 1.3) $M_\odot$ from the main sequence to the red giant branch, where mass exchange can begin, of about ∼6 and ∼5 Gyr, respectively.

From the other side, we calculated the galactic orbit of AU Peg based on astrometric data from Gaia DR3 in three-component Galaxy potential model (https://gravpot.utinam.cnrs.fr/). AU Peg orbit is enclosed in an orbital torus with the height $|z| \leq 0.3$ kpc and inner and outer distances of 7.2–8.8 kpc from the galactic center. Rotation velocity of the system varies within (225–255) km/s, the vertical velocity $|V_z| \leq 18$ km/s; these kinematic parameters are characteristic of the population of

the thin/old disk of the Galaxy. Therefore, based on a combination of characteristics – belonging to the disk population of the Galaxy in both position and kinematics, nearly solar metallicity $[Fe/H] \geq -0.20$, a complicated evolutionary history with mass exchange – AU Peg seems to be very different from "typical" BL Her subtype star. Moreover, no evolutionary calculations (Das et al. 2021, 2024; Marconi and Di Criscienzo 2007) match the set of physical parameters of this star. Obviously, the current evolution and pulsation statuses of AU Peg need further study.

2.3 T2 Cepheid TX Del

The variability of TX Del (Gaia DR3 1734124248699204096) was discovered by Hoffmeister (1935). As part of a large-scale photometric study of 184 Cepheids in two colors, Walraven et al. (1958) noted the possible affiliation of TX Del to T2 Cepheids, and Petit (1960), based on its position in the Galaxy, assigned it to the T2 population with certainty. TX Del was included in the catalog of type II Cepheids by Harris (1985). TX Del, the second spectroscopic binary Cepheid after AU Peg by the orbital period of approximately $P_{orb} \sim 133^d$, usually classified as a BL Her subtype, has properties not quite typical for stars of this class. First, the chemical composition is more typical of thin or old disk stars; second, Vinko et al. (1998) noted that estimates of its radius estimates (∼40–60 $R_\odot$) are too large for T2 Cepheids and are more typical of classical Cepheids of the same pulsation period, $P_{pls} \approx 6.1662^d$. Bohm-Vitense and Proffitt (1985) from the UV flux from TX Del companion, observed by IUE satellite in the spectral range of 100–200 nm, set an upper limit on its temperature and mass: $T_{\rm eff} < 8200$–8500 K, $M/M_\odot < 2.1$–2.2.

As for the case of AU Peg, we decided to revise the status of TX Del Cepheid using the same approach: radial velocities, Gaia DR3 photometric and astrometric data. Orbit calculations give the values of mass function $f(M) \approx 0.036 \pm 0.002$ and separation $a_1 \cdot \sin\ i \approx 0.169 \pm 0.003$. The radius was calculated for different values of the projection factor PF ranging from 1.24 to 1.34, with mean radius value of $\langle R/R_\odot \rangle \approx 20.6 \pm 0.6$ and variation amplitude of ± 1 $R_\odot$. Based on the Bayesian distance estimate of Bailer-Jones et al. (2021), we estimated the absolute magnitudes of TX Del Cepheid as $\langle M_V \rangle_I \approx -1.31 \pm 0.05$ mag, $\langle M_G \rangle_I \approx -1.40 \pm 0.03$ mag. So, the radius and luminosity of TX Del were found to be significantly smaller than those of classical Cepheids of the same period and are consistent with the "period–luminosity" (Clementini et al. 2016, Ripepi et al. 2019) and "period–radius" (Groenewegen and Jurkovic 2017) relations for T2 Cepheids. Summarizing the results obtained only about the pulsation radius and luminosity, we could assign TX Del to the subtype of BL Her variables.

The relationship between the masses of the main component M_1 and the companion M_2 for orbital plane inclination angles $i = (20, 30, 40, 50, 60, 70)^\circ$ is shown in the upper left panel of Fig. 4. The lower black dashed line (almost matching the line for the inclination angle $i \approx 70^\circ$) bounds the "forbidden region" of mutual eclipses assuming that the companion is a main-sequence star. The upper dashed line corresponds to $M_2 = 2$ $M_\odot$, i.e., the upper limit on the companion mass imposed by the UV observations. The companion's contribution to the brightness of the total system does not exceed 6–7% (Mamajek 2022). The upper right panel shows the mass ratio $q = M_1/M_2$ for different tilt angles (the horizontal dashed line indicates mass

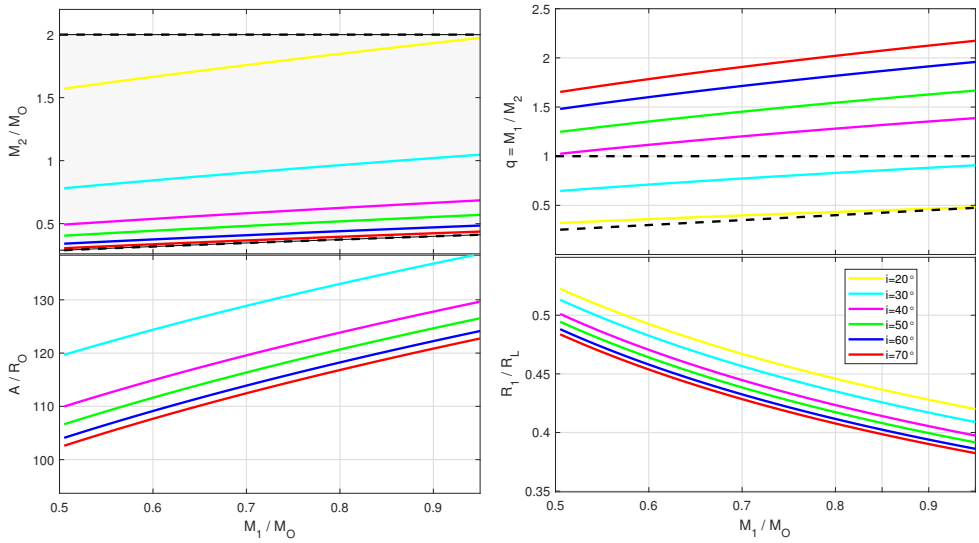


Figure 4 Diagnostic diagrams for TX Del. Dependencies of parameters – satellite mass M_2, mass ratio $q = M_1/M_2$, degree of filling of the Roche lobe R_1/R_L by the main component, distance between components $A/R_\odot$ – on the mass of the Cepheid M_1 for the tilt angles $i = (20, 30, 40, 50, 60, 70)^\circ$. The lower black dashed line in the upper left panel limits the "forbidden zone" in which mutual eclipses of the components are possible; the upper dashed line – the maximum companion mass 2 $M_\odot$ (constraint taken from its UV flux contribution). Horizontal dashed line in the upper right panel marks the line $M_1 = M_2$.

equality, the inclined dashed line corresponds to $M_2 = 2\ M_\odot$). The lower left and right panels show estimates of the separation between the components $A/R_\odot$ and the degree of filling of the Roche sphere R_1/R_L with the principal component for different tilt angles, respectively. In Fig. 4, it can be seen that the Cepheid fills the Roche lobe by about 37–55%, depending on the mass and inclination angle assumed.

Analysis of the diagnostic diagrams shows that for all given values of the TX Del mass of the main component, the orbit inclination angles lie within the range ∼20–70°. For inclination angles greater than approximately 35–40°, the mass of the main component being higher than the companion mass. Solutions with a companion mass higher than the mass of the main component are possible at inclination angles approximately from ∼ 20° to 30–35°. In the latter case, the lower mass of the Cepheid can be explained by the inevitable mass transfer in the binary system from the initially more massive star that has evolved to the companion, a main-sequence star.

Using the *rgeo* distance estimate, Gaia DR3 proper motion and the radial velocity of the system's center of mass V_γ, we calculated the Galactic orbit parameters of TX Del, as for AU Peg star (https://gravpot.utinam.cnrs.fr/). The orbit is enclosed in an orbi tal torus with the height of $|z| \leq 0.42$ kpc, and with inner and outer orbit radii of 7.2–8.3 kpc. The rotation velocity of the system varies within (220–255) km/s, the vertical velocity $|V_z| \leq 38$ km/s. These parameters are very similar to that of AU Peg Cepheid. It is extremely interesting that calculations of the galactic orbital parameters of the prototype of the subclass – the Cepheid BL Her itself – using Gaia DR3

astrometric data give similar results: an orbital torus of thickness $|z| \leq 0.40$ kpc with inner and outer radii of 6.3–8.5 kpc, rotation velocity of (205–270) km/s, vertical velocity in the range ±40 km/s, and orbital period of about 200 My. In terms of kinematic characteristics, BL Her also appears to be representative of the population of an old disk with an exponential scale on the order of $H_z \sim 0.3$ kpc.

Based on the chemical composition, $[Fe/H] \geq +0.10$, position in the Galaxy, and kinematic characteristics, TX Del can be confidently assigned to the old disk (8-10 Gyr old). The MESA (Dotter 2016) evolutionary tracks predict an evolutionary time to the red giant stage on the order of 11.3 Gyr for a solar-mass star, and a time of about 9.5 Gyr for a star with an initial mass of 1.05 $M_\odot$. Consequently, the initial mass of the main component must have been at least 1.05–1.10 $M_\odot$ for the star to evolve to the low-mass subgiant or mass exchange stage.

3 Conclusion

The combined use of the photometry, spectroscopy (radial velocities), and high-precision astrometric data from Gaia DR3 (distances and proper motions) makes it possible to study the spectroscopic binary Cepheids with unprecedented detail. An important role is played by estimates of the pulsation radii, one of the main stellar parameters, and the possibility to set the additional constraints on the masses of binary components and their evolutionary status.

We have seen that two BL Her-type Cepheids – AU Peg and TX Del – show photometric properties (periods and luminosities) characteristic for stars of this type, including population of variable stars in metal-deficient globular clusters. On the contrary, their chemical composition, galactic position and the parameters of their galactic orbits bring them closer to typical objects of thin/old disk populations. It is also worth mentioning that the set of astrophysical parameters of AU Peg and TX Del (and probably a number of other similar variables) is not fully described by existing evolutionary and pulsation theoretical calculations. The membership in binary systems and mass exchange processes obviously play an important role. Additional evolutionary and pulsation calculations over a wider range of periods, luminosities, radii and chemical composition are required to definitively clarify the evolutionary status of such variables.

Acknowledgements

The study was conducted under the state assignment of Lomonosov Moscow State University. The authors are grateful to the participants of the multi-year program of measuring radial velocities: M.E. Sachkov (INASAN), E.V. Glushkova (MSU), A.A. Fedorova (IKI RAS). This work has made use of data from the European Space Agency (ESA) mission *Gaia* (https://www.cosmos.esa.int/gaia), processed by the *Gaia* Data Processing and Analysis Consortium (DPAC, https://www.cosmos.esa.int/web/gaia/dpac/consortium). Funding for the DPAC has been provided by national institutions, in particular the institutions participating in the *Gaia* Multilateral Agreement.

Conflict of interests

The authors declare the absence of conflict of interest.

References

C. A. L. Bailer-Jones, J. Rybizki, M. Fouesneau, et al., Astron. J. **156** (2), 58 (2018).
C. A. L. Bailer-Jones, J. Rybizki, M. Fouesneau, et al., Astron. J. **161** (3), 147 (2021).
L. A. Balona, Monthly Notices Royal Astron. Soc. **178**, 231 (1977).
T. G. Barnes and D. S. Evans, Monthly Notices Royal Astron. Soc. **174**, 489 (1976).
T. G. Barnes, D. S. Evans, and T. J. Moffett, Monthly Notices Royal Astron. Soc. **183**, 285 (1978).
E. Bohm-Vitense and C. Proffitt, Astrophys. J. **296**, 175 (1985).
A. M. Cherepashchuk, *Tesnye Dvoynye Zvezdy, Vol. I* (2013).
G. Clementini, V. Ripepi, S. Leccia, et al., Astron. and Astrophys. **595**, A133 (2016).
S. Das, S. M. Kanbur, R. Smolec, et al., Monthly Notices Royal Astron. Soc. **501** (1), 875 (2021).
S. Das, L. Molnar, S. M. Kanbur, et al., Astron. and Astrophys. **684**, A170 (2024).
A. Dotter, Astrophys. J. Suppl. **222** (1), 8 (2016).
N. Evans, A Precision Measurement of the Mass of the Cepheid V350 Sgr, HST Proposal ID 13368. Cycle 21 (2013).
N. R. Evans, L. Berdnikov, N. Gorynya, et al., Astron. J. **142** (3), 87 (2011).
N. R. Evans, E. Bohm-Vitense, K. Carpenter, et al., Publ. Astron. Soc. Pacific 109, 789 (1997).
N. R. Evans, C. Proffitt, K. G. Carpenter, et al., Astrophys. J. **866** (1), 30 (2018).
N. R. Evans and B. J. A. Sugars, Astron. J. **113**, 792 (1997).
Gaia Collaboration, A. G. A. Brown, A. Vallenari, et al., Astron. and Astrophys. **616**, A1 (2018).
Gaia Collaboration, A. G. A. Brown, A. Vallenari, et al., Astron. and Astrophys. **649**, A1 (2021).
Gaia Collaboration, T. Prusti, J. H. J. de Bruijne, et al., Astron. and Astrophys. **595**, A1 (2016).
Gaia Collaboration, A. Vallenari, A. G. A. Brown, et al., Astron. and Astrophys. **674**, A1 (2023).
N. A. Gorynya, T. R. Irsmambetova, A. S. Rastorgouev, and N. N. Samus, Soviet Astronomy Letters **18**, 316 (1992).
N. A. Gorynya, N. N. Samus, L. N. Berdnikov, et al., Information Bulletin on Variable Stars **4199**, 1 (1995).
N. A. Gorynya, N. N. Samus', A. S. Rastorguev, and M. E. Sachkov, Astronomy Letters **22** (2), 175 (1996).
N. A. Gorynya, N. N. Samus', M. E. Sachkov, et al., Astronomy Letters **24** (6), 815 (1998).
M. A. T. Groenewegen and M. I. Jurkovic, Astron. and Astrophys. **604**, A29 (2017).
H. C. Harris, Astron. J. **90**, 756 (1985).
H. C. Harris, E. W. Olszewski, and G. Wallerstein, Astron. J. **89**, 119 (1984).

C. Hoffmeister, Astronomische Nachrichten **240**, 193 (1930).
C. Hoffmeister, Astronomische Nachrichten **255**, 401 (1935).
E. E. Mamajek, A Modern Mean Dwarf Stellar Color and Effective Temperature Sequence, https:// www.pas.rochester.edu/emamajek/EEM_dwarf_UBVIJHK_colors_Teff.txt (last updated April 16, 2022).
M. Marconi and M. Di Criscienzo, Astron. and Astrophys. **467** (1), 223 (2007).
M. Petit, Annales d'Astrophysique **23**, 710 (1960).
A. S. Rastorguev and A. K. Dambis, Astrophysical Bulletin **66** (1), 47 (2011).
A. S. Rastorguev, M. V. Zabolotskikh, and N. A. Gorynya, Astronomy Reports **68** (12), 1457 (2024a).
A. S. Rastorguev, M. V. Zabolotskikh, and N. A. Gorynya, Astrophysical Bulletin **79** (4), 629 (2024b).
A. S. Rastorguev, M. V. Zabolotskikh, Y. A. Lazovik, et al., Astrophysical Bulletin **77** (2), 144 (2022).
V. Ripepi, R. Molinaro, I. Musella, et al., Astron. and Astrophys. **625**, A14 (2019).
I. Soszyński, A. Udalski, M. K. Szymanski, et al., Acta Astronomica **67** (2), 103 (2017a).
I. Soszyński, A. Udalski, M. K. Szymanski, et al., Acta Astronomica **67** (4), 297 (2017b).
I. Soszyński, A. Udalski, M. K. Szymanski, et al., Acta Astronomica **68** (2), 89 (2018).
A. A. Tokovinin, Sov. Astron. **31**, 98 (1987).
A. Udalski, M. K. Szymanski, and G. Szymanski, Acta Astronomica **65** (1), 1 (2015).
J. Vinko, N. Remage Evans, L. L. Kiss, and L. Szabados, Monthly Notices Royal Astron. Soc. **296** (4), 824 (1998).
J. Vinko, L. Szabados, and K. Szatmary, Astron. and Astrophys. **279**, 410 (1993).
T. Walraven, A. B. Muller, and P. T. Oosterhoff, Bull. Astron. Inst. Netherlands **14**, 81 (1958).